Supporting Information

Incorporating paraffin@SiO_2 nanocapsules with abundant surface hydroxyl groups into polydimethylsiloxane to develop composites with enhanced interfacial heat conductance for chip heat dissipation

Shushan Li[†‡], Zekai Lin[†‡], Zezhi Zhou[†‡], Yu Zhao[†‡], Ziye Ling[†‡], Zhengguo Zhang[†‡], Xiaoming Fang[†‡*]

[†] Key Laboratory of Enhanced Heat Transfer and Energy Conservation, The Ministry of Education, School of Chemistry and Chemical Engineering, South China University of Technology, Guangzhou 510640, China.

[‡] Guangdong Engineering Technology Research Center of Efficient Heat Storage and Application, South China University of Technology, Guangzhou 510640, China.

[*]Corresponding author, Tel: 86 20 87112997, Fax: 86 20 87113870, Email: cexmfang@scut.edu.cn.

S1 Materials:

Paraffin with a melting point of 44 ℃ was purchased from Guangzhou Zhongjia New Material Technology Co., LTD. Co., Ltd. Tetraethoxysilane (TEOS, CP), hydrochloric acid (HCl, AR, 36-38%) and 25% of an ammonia solution ($NH_3 \cdot H_2O$, analytically pure, AR) were purchased from Guangzhou Chemical Reagent Factory. Anhydrous ethanol (AR), formamide (AR), petroleum ether (AR) and n-hexane (C_6H_{14}, AR) were purchased from Tianjin Fuyu Fine Chemical Co., Ltd. Cetyltrimethylammonium bromide (CTAB, 99%) was purchased from Shanghai Boao Biotechnology Co., Ltd. Hexagonal boron nitride (BN, 5~10 μm in size and 250~400 nm in thickness) was obtained from Minnesota Mining and Manufacturing Co., Ltd., USA. Sylgard 184 silicone elastomer (consisting of a base and a curing agent at a weight ratio of 10:1), a common polydimethylsiloxane (PDMS) prepolymer kit, was purchased from Dow Corning, which was used as the matrix for preparing the composites. All reagents were used as received without further purification.

S2 Preparation of paraffin@SiO_2 phase change microcapsules (PCMCs)

The PCMCs were prepared by the following process[1]. In a typical procedure, 2.25 g of CTAB was dissolved in 141 mL of formamide to obtain a homogeneous solution, and then the solution was transferred into a 250 mL three-neck round-bottom flask. Subsequently, 15 g of Paraffin and 10 g of TEOS were added into the flask, followed by mixing at 60 ℃ with stirring at a rate of 350 rpm for 4 h to form a nonaqueous O/W emulsion. Then, 48 mL of an HCl aqueous solution (1 mol/L) was added slowly to the emulsion with vigorous agitation for 16 h, followed by aging at 60 °C for 12 h. Finally, the paraffin@SiO_2 PCMCs were obtained by filtration and washing with deionized water, ethanol, and petroleum ether several times in sequence, and dried at room temperature overnight.

S3 Characterizations and measurements

The morphologies and microstructures of the paraffin@SiO_2 phase change nanocapsules (PCNCs) and PCMCs, the PDMS-based composites as well as the composites were observed on a field emission scanning electron microscopy (SEM, SU8220, HITACHI). Particle size distribution analysis was performed on the PCNCs by using a laser particle size meter (BT-9300LD). The microstructures of the synthesized nanocapsules were determined by TEM using a Hitachi H-800 transmission electron microscope operating at an accelerating voltage of 100 kV (TEM, H-800, HITACHI).

The phase change temperatures and enthalpy values of the samples were characterized using a differential scanning calorimeter (DSC, Q20, TA). For DSC measurements, 5-10 mg for every sample was sealed within an aluminum pan for characterization, heating from 20 °C to 70 °C and then cooling to 20 °C at a rate of 10 °C·min^{-1} under a constant stream of nitrogen at a flow rate of 50 mL·min^{-1}. Additionally, the thermal reliability of the samples was evaluated by making them experience the heating-cooling cycle tests, followed by the DSC measurement. The thermal stabilities of the samples were measured using a thermogravimetric analyzer (TGA, STA6000, PerkinElmer., USA) within the range of 40-400℃ under air atmosphere.

The thermal conductivities of the PDMS-based composites were measured on a thermal constant analyzer (Hot Disk, TPS 2500, Sweden) at room temperature (25℃). The measuring time was 10 s, and the heating power was controlled at 10-30 mW. The sensor was sandwiched between two pads made of the same sample, and at least four parallel samples were prepared for each measurement to ensure the repeatability of the results.

The Fourier transform infrared spectroscopy (FT-IR) spectra were recorded on a Nicolet IS50 Fourier transform infrared spectrometer (Thermo Fisher Scientific) from 4000 cm^{-1} to 400 cm^{-1}

with 32 scans using KBr pellets. Variable temperature FTIR spectra were tested from 30 to 150 °C. Moreover, based on ASTM E168-16 standard, a quantitative analysis of the FT-IR spectrum was performed as follows:

According to the Lambert-Beer Law Eq. (2)[2]:

$$A=\varepsilon\times c\times l$$

Where A is absorbance, ε is a characteristic of the material called the extinction coefficient affected by wavelength and temperature, c is the concentration of the material in an appropriate unit, and l is the thickness of the material. Accordingly, for a given wavelength, temperature and thickness, ε and l are constants, the absorbance (A) is proportional to the concentration (c).

Solid-state NMR studies were performed with a Bruker AvanceII spectrometer operating at 600 MHz Lamor frequency.

Surface chemical states were investigated by X-ray photoelectron spectroscopy (XPS) measurement with Thermo Scientific ESCALAB 250Xi system by Al Karadiation and adventitious C1s peak (284.6 eV) as the reference.

The X-ray diffraction (XRD) patterns of the samples were taken on an X-ray diffractometer (Rigaku, SmartLab) by scanning the 2θ range from 10° to 60°.

The hardness values of the PDMS-based composites were measured by a hardness tester (Digital Shore Durometer, Model A, SYATEK).

The mechanical properties of the PDMS-based composites were tested on an electronic universal testing machine at a crosshead speed rate of 5 mm/min.

The volume resistivity was measured using a high resistance meter (Keithley 6517B, Tektronix Inc., USA) to explore the insulating property of the composites.

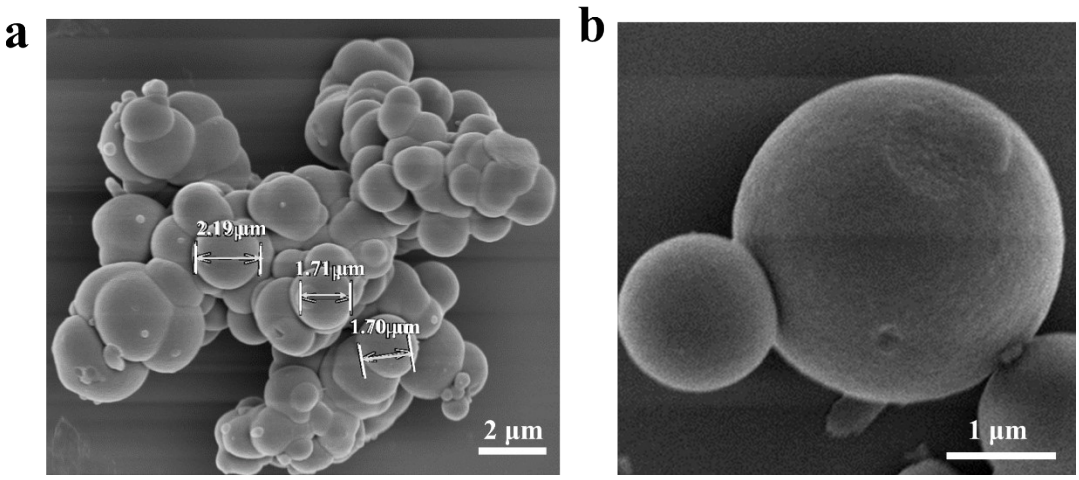

Figure S1 SEM images of the PCMCs (a, b).

Table S1 Comparisons in phase change characteristics between PCNCs and PCMCs.

Samples	T_m (°C)	ΔH_m (J·g^{-1})	T_f (°C)	ΔH_f (J·g^{-1})	E (%)
PCNCs	42.10	176.5	43.19	172.9	74.29
PCMCs	41.33	160.2	43.88	157.2	67.49

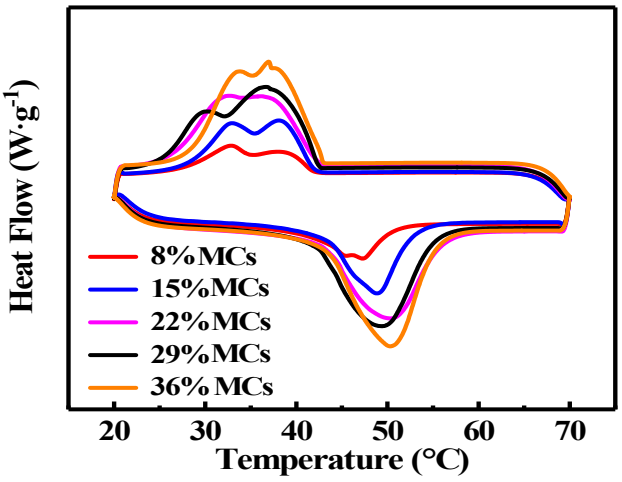

Figure S2 DSC curves of the PDMS-based composites containing different mass fractions of the

PCMCs.

Table S2 Phase change characteristics of the PDMS-based composites

Samples	T_m (°C)	ΔH_m (J·g^{-1})	T_f (°C)	ΔH_f (J·g^{-1})
8%MCs	43.88	11.80	43.98	10.02
15%MCs	44.02	23.00	43.59	21.99
22%MCs	44.13	35.24	43.58	33.88
29%MCs	43.98	46.08	43.33	45.12
36%MCs	44.18	56.46	43.78	55.98

containing different mass fractions of the PCMCs.

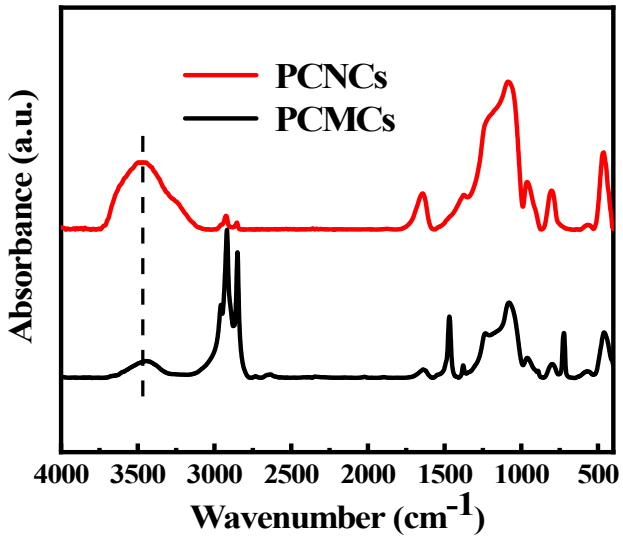

Figure S3 FT-IR absorbance-wavelength curves of PCNCs and PCMCs

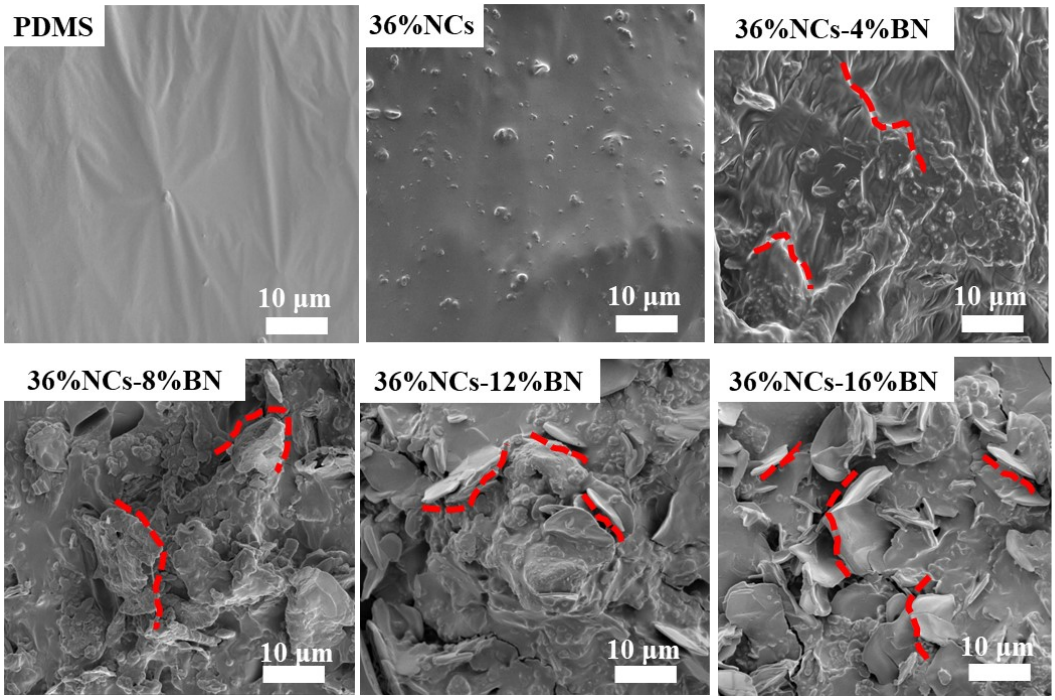

Figure S4 SEM images of the PDMS matrix and the PDMS-based composites containing different mass fractions of the PCNCs and BN (red lines denote the BN).

Table S3 Phase change characteristics of the PDMS-based composites containing both the PCNCs and the BN sheets.

Samples	**PCNCs (wt%)**	**BN (wt%)**	T_m (°C)	ΔH_m (J·g^{-1})	T_f (°C)	ΔH_f (J·g^{-1})
36% NCs	36	0	43.38	63.59	44.58	62.19
36%NCs-4%BN	36	4	42.50	63.39	44.19	62.39
36%NCs-8%BN	36	8	41.73	63.38	44.38	61.98
36%NCs-12%BN	36	12	41.23	63.47	43.98	62.09
36%NCs-16%BN	36	16	41.02	63.59	44.22	62.30

Reference

[1] H. Zhang, S. Sun, X. Wang, D. Wu, Fabrication of microencapsulated phase change materials based on n-octadecane core and silica shell through interfacial polycondensation, Colloids and Surfaces A: Physicochemical and Engineering Aspects, 389 (2011) 104-117.
[2] Y.S. Lee, W.-K. Lee, S.-G. Cho, I. Kim, C.-S. Ha, Quantitative analysis of unknown compositions in ternary polymer blends: A model study on NR/SBR/BR system, Journal of Analytical and Applied Pyrolysis, 78 (2007) 85-94.